Title
Med12 regulates ovarian steroidogenesis, uterine development and maternal effects in the mammalian egg

Journal
Biology of Reproduction, 97(6)

ISSN
0006-3363

Authors
Wang, Xinye
Mittal, Priya
Castro, Carlos A
et al.

Publication Date
2017-12-31

DOI
10.1093/biolre/iox143

Biology of Reproduction, 2017, 97(6), 822–834
doi:10.1093/biolre/iox143
Research Article
Advance Access Publication Date: 8 November 2017

Research Article

Med12 regulates ovarian steroidogenesis, uterine development and maternal effects in the mammalian egg†

Xinye Wang[1,2], Priya Mittal[3,4], Carlos A. Castro[2], Gabriel Rajkovic[2] and Aleksandar Rajkovic[2,3,5,*]

[1]Tsinghua MD Program, Tsinghua University School of Medicine, Beijing, China; [2]Department of Obstetrics, Gynecology and Reproductive Sciences, Magee-Womens Research Institute, Pittsburgh, Pennsylvania, USA; [3]Department of Human Genetics, Graduate School of Public Health, University of Pittsburgh, Pittsburgh, Pennsylvania, USA; [4]Department of Oncology, St. Jude Children's Research Hospital, Memphis, Tennessee, USA and [5]Department of Pathology, University of Pittsburgh, Pittsburgh, Pennsylvania, USA

****Correspondence:** Department of Obstetrics, Gynecology and Reproductive Sciences, Magee-Womens Research Institute, 204 Craft Avenue-A224, Pittsburgh, PA 15213, USA. Tel: 412.641.8635; E-mail: rajkovica2@mail.magee.edu

†**Grant support:** This work was supported in part by grants from Magee Womens Research Institute and R01 HD088629 to AR. XW was supported by a China Scholarship Council award through Tsinghua University School of Medicine and Tsinghua-Pittsburgh Joint Program.

Received 1 August 2017; Revised 2 October 2017; Accepted 7 November 2017

Abstract

The transcriptional factor MED12 is part of the essential mediator transcriptional complex that acts as a transcriptional coactivator in all eukaryotes. Missense gain-of-function mutations in human *MED12* are associated with uterine leiomyomas, yet the role of *MED12* deficiency in tumorigenesis and reproductive biology has not been fully explored. We generated a *Med12* reproductive conditional knockout mouse model to evaluate its role in uterine mesenchyme, granulosa cells, and oocytes. Mice heterozygous for *Med12* deficiency in granulosa cells and uterus (*Med12*$^{fl/+}$ *Amhr2-Cre)* were subfertile, while mice homozygous for *Med12* deficiency in granulosa cells and uterus (*Med12*$^{fl/fl}$ *Amhr2-Cre*) were infertile. Morphological and histological analysis of the *Med12*$^{fl/fl}$ *Amhr2-Cre* reproductive tract revealed atrophic uteri and hyperchromatic granulosa cells with disrupted expression of *Lhcgr, Esr1*, and *Esr2*. *Med12*$^{fl/fl}$ *Amhr2-Cre* mice estrous cycle was disrupted, and serum analysis showed blunted rise in estradiol in response to pregnant mare serum gonadotropin. Uterine atrophy was partially rescued by exogenous steroid supplementation with dysregulation of *Notch1* and *Smo* expression in steroid supplemented *Med12*$^{fl/fl}$ *Amhr2-Cre* uteri, indicating intrinsic uterine defects. Oocyte-specific ablation of *Med12* caused infertility without disrupting normal folliculogenesis and ovulation, consistent with maternal effects of *Med12* in early embryo development. These results show the critical importance of *Med12* in reproductive tract development and that *Med12* loss of function does not cause tumorigenesis in reproductive tissues.

Summary Sentence

Med12 conditional deficiency causes uterine, ovarian and post-fertilization dysfunction and infertility.

Key words: Med12, uterus, ovary, infertility.

Introduction

Mediator complex functions as a transcriptional coactivator in all eukaryotes [1]. Mediator complexes interact with transcription factors and RNA polymerase II. One of the main functions of mediator complexes is to transmit signals from the transcription factors to the polymerase. MED12 protein is part of a kinase module of the mediator complex that modulates transcriptional regulation of RNA polymerase II complex [1, 2]. MED12 is highly conserved among eukaryotes [3]. *MED12* gene is located on the X chromosome and encodes a 250-kDa protein that is ubiquitously expressed during embryonic development and beyond [4]. MED12, MED13, CDK8, and Cyclin C proteins constitute the kinase module of the mediator complex and can act as transcriptional activator or repressor [5, 6]. MED12 protein is also critical for the kinase activity of CDK8 [7]. Multiple pathways, such as sonic hedgehog and estrogen receptors, are known to interact with MED12 [8–10]. *Med12* genetic studies in vivo indicate that *Med12* is essential for early embryo development, as *Med12* hypomorphic mutation is lethal in mouse embryos [11]. In humans, *MED12* germline mutations have been associated with mental retardation syndromes [9], while somatic mutations have been associated with tumorigenesis. For example, *MED12* exon 2 variants were present in 59% of fibroadenomas, 80% of phyllodes tumors [12–15], and in 5% of hormone-related prostate and 5% of adrenocortical carcinomas [16, 17]. Moreover, almost 70% of uterine leiomyomas carry exon 2 *MED12* mutations [18, 19]. In leiomyomas, these associations are likely causative, as exon 2 *MED12* mutations induce uterine tumors in mice via a gain-of-function mechanism [20]. However, the effects of *MED12* deficiency on reproductive tract development and tumorigenesis are unknown.

We investigated the effects of loss-of-function mutations on the reproductive tract function. We generated mice to induce conditional deficiency of *Med12* in the reproductive tract by crossing *Med12* floxed animals with anti-Mullerian receptor II Cre (*Amhr2-Cre*), growth differentiation factor 9 Cre (*Gdf9-Cre*), and zona pellucida glycoprotein 3 Cre (*Zp3-Cre*) animals. The various mouse models allowed us to study the effects of *Med12* deficiency on mouse granulosa cells, uterine mesenchyme, and oocytes. Our results indicate that *Med12* loss of function does not cause tumorigenesis, and that *Med12* acts as a maternal effect gene, while in the somatic compartment, *Med12* deficiency causes infertility by disrupting uterine development and ovarian steroidogenesis.

Methods

Experimental mice

The University of Pittsburgh Institutional Animal Care and Use Committee approved the study. We followed University of Pittsburgh and NIH guidelines to ensure the well-being and humane treatment of the animals. The $Med12^{fl/fl}$ mice were kindly provided by Dr Heinrich Schrewe [11]. Dr Richard Behringer generously provided the anti-Mullerian hormone type 2 receptor, targeted mutation 3 transgenic mice ($Amhr2^{tm3(cre)Bhr}$) which we used in heterozygous state under the synonymous nomenclature *Amhr2-cre* [21]. All mice were housed under 12 h light and 12 h dark per day and provided food and water ad libitum. Genotyping of mice was conducted on tail DNA using standardized PCR protocols [11].

Fertility and mating tests

Fertility studies were performed by housing a single female with a proven male stud for at least 6 months, during which data on litter size, number of litters per month, and offspring gender were collected. At least five females of each genotype were used to determine fertility and to compare with appropriate controls. For the mating study, estrous-synchronized females (5 IU PMSG for 48 h followed by 5 IU hCG for 20 h) were housed with proven stud males overnight. Examination of vaginal plugs was conducted on the following morning, and the males were separated from the females at the same time. The presence of plugs was determined at 0.5 days postconception.

Estrous cycle stages were assessed on mice at 40 days of age by performing and analyzing vaginal smears. Cotton balls dipped in 0.9% saline were used to first clean the vaginal opening. About 20 μl saline was flushed into the vagina by plastic pipette four to five times. The effluent was examined on a glass slide under light microscope. The four stages (proestrus, estrus, metestrus, and diestrus) were scored on the basis of the vaginal smears as previously described [22].

Ovarian and uterine histological analysis

Before harvesting the uteri from euthanized mice at age greater than 6 weeks, all mice were synchronized by 5 IU PMSG for 48 h, followed by 5 IU hCG for 20 h. The uteri were then fixed in 10% formalin overnight, embedded in paraffin, sectioned at a thickness of 6 μm, and stained with hematoxylin & eosin for further interpretation. For ovarian histological analysis, ovaries were collected from mice of various ages. The collected ovaries were then fixed in 10% formalin overnight, embedded in paraffin, serially sectioned to a thickness of 5 μm, and processed by periodic acid–Schiff staining.

Ovarian follicle counting was performed on serial sections along the long axis of the ovaries stained by periodic acid-Schiff staining. Every fifth section was counted. Only follicles where oocyte nuclei were visualized were scored. The mean of total scored follicles from all counted sections was considered as the number of follicles per ovary. Ovarian follicle types were defined as previously described [23].

Serum hormone analysis

For estradiol and progesterone quantitation, the serum samples were processed at the Ligand Assay & Analysis Core, Center for Research in Reproduction, School of Medicine, University of Virginia.

RNA isolation and real-time PCR

Three-week-old mice were synchronized by 5 IU PMSG for 48 h before being euthanized. Ovaries were removed, and large follicles were punctured to collect granulosa cells in 1 ml granulosa collection culture (DME-F12, 1X penicillin-streptomycin, 0.3% BSA, 10 mM Hepes), using two 26-G needles. The cellular suspension was cleaned by a 40-μm nylon filter, followed by an enriching step (1000 g, 10 min), to get granulosa cell pellets. RNA was extracted from the cell pellets using TRIzol reagent. The primers were customized using the Integrated DNA Technologies Web tool (Supplementary Table S1). The quantitative real-time PCR was conducted in a SYBR Green detection system (Bio-Rad CFX96 PCR Detection System). The data were normalized against *Gapdh*, and the relative mRNA was calculated by applying $2^{-\Delta\Delta CT}$ methods [24].

Steroid pellet implantation and uterine studies

Four-week-old mice were anesthetized by 3% isoflurane and were administered 5 mg/kg Rimadyl (Zoetis) and 0.1 mg/kg buprenorphine (Patterson Veterinary) for analgesic purposes. A 3 × 3 cm area on the back of mice was shaved and sterilized with alcohol swab (BD Medical Technology) and iodine pads (Medline Industries). The ovaries were exteriorized and removed via posterior

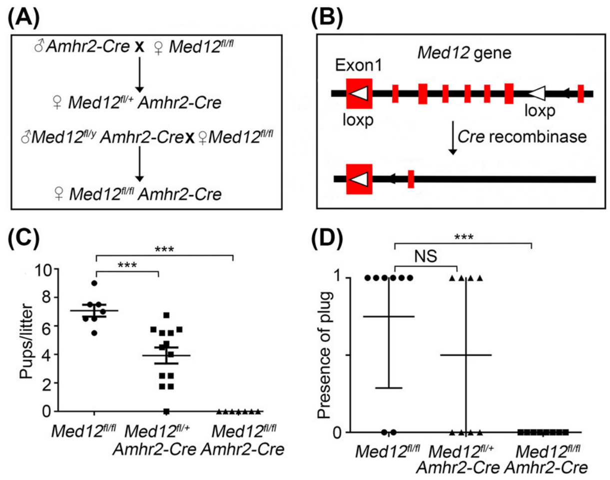

Figure 1. *Med12$^{fl/fl}$ Amhr2-Cre* female mice are infertile. (A) Breeding crosses used to generate *Med12$^{fl/fl}$ Amhr2-Cre* and *Med12$^{fl/y}$ Amhr2-Cre* mice for experimental studies. (B) Schematic representation of floxed *Med12* allele. LoxP sites bracket exons 1–7 of the *Med12* gene. In *Amhr2-Cre* transgenic mice, *Amhr2* promoter drives *Cre* expression in uterine mesenchyme, oviduct, and granulosa cells of ovaries. (C) Fertility data of control (*Med12$^{fl/fl}$*) (n = 7), *Med12$^{fl/+}$ Amhr2-cre* (n = 13), and *Med12$^{fl/fl}$ Amhr2-cre* (n = 7) female mice. The mice were bred with wild-type stud males for 6 months. (D) Mating success was evaluated by vaginal plug detection (n = 8). Data are presented as mean ± SEM. $^{***}P < 0.001$ (C, D).

incision. Estradiol pellets (0.5 mg/pellet, 90-day release, Innovative Animal Research) and progesterone pellets (25 mg/pellet, 90-day release, Innovative Animal Research) were implanted in the subcutaneous space towards the lateral sides of the mouse neck. After 4 weeks of implantation, the mice were euthanized for further analysis.

Statistics

Two-tailed Student *t* test and two-way ANOVA were applied to determine the significance between control and experimental groups. A *P* value less than 0.05 was considered statistically significant. Data were plotted and analyzed by GraphPad Prism 6.

Results

Med12 is essential for female fertility

We generated *Med12* conditional knockout mice to study the effects of *Med12* deficiency on ovarian granulosa and uterine mesenchymal somatic cells by crossing *Amhr2-Cre* and *Med12$^{fl/fl}$* mice (Figure 1A). The *Med12$^{fl/fl}$* animals have exons 1 through 7 floxed, and in the presence of a well-characterized *Amhr2-Cre* [20], uterine mesenchyme and ovarian granulosa cells lose *Med12* expression (Figure 1B). We previously determined that 60% of cells underwent *Amhr2-Cre*-mediated recombination in the reproductive tract [20]. We examined fertility in animals with one floxed *Med12* allele (heterozygous) in the presence of *Amhr2-Cre* (*Med12$^{fl/+}$ Amhr2-Cre*), two floxed *Med12* alleles (homozygous) in the presence of *Amhr2-Cre* (*Med12$^{fl/fl}$ Amhr2-Cre*), and controls (*Med12$^{fl/fl}$*). The females were bred with wild-type males for 6 months, and the number of pups per litter was recorded. *Med12$^{fl/+}$ Amhr2-Cre* females were subfertile, producing on average 4 ± 0.5 pups per litter, as compared to the controls 7 ± 1.5 pups per litter (n = 7, $P < 0.001$, Figure 1C). *Med12$^{fl/fl}$ Amhr2-Cre* females were infertile (n = 7, $P < 0.001$, Figure 1C).

We assessed the mating behavior of *Med12$^{fl/+}$ Amhr2-Cre* and *Med12$^{fl/fl}$ Amhr2-Cre* females by monitoring vaginal plugs in the presence of stud males. *Med12$^{fl/fl}$ Amhr2-Cre* females lacked vaginal plugs, while *Med12$^{fl/+}$ Amhr2-Cre* and control females had equal number of vaginal plugs (n = 8, $P < 0.001$, Figure 1D). These results indicated abnormal sexual behavior in *Med12$^{fl/fl}$ Amhr2-Cre* females.

Med12$^{fl/y}$ Amhr2-Cre males were subfertile producing on average 5 ± 0.5 pups per litter (n = 7, $P < 0.05$, Supplementary Figure 1A), indicating that *Med12* is not as critical in the biology of steroid producing Sertoli and Leydig cells [25].

Med12 disrupts estrous cyclicity

We examined vaginal secretions in the *Med12$^{fl/fl}$ Amhr2-Cre* females to assess the estrous cycle to understand why mating did not occur. We monitored the time of onset of vaginal cornification, the age of first onset of estrous cycle, the number of estrous cycles occurring, and the time spent in each stage of the estrous cycle during the 6-week period. Estrous cycle in rodents is divided into four stages including proestrus, estrus, metestrus, and diestrus stage. The representative estrous stages of control and *Med12$^{fl/fl}$ Amhr2-Cre* mice are shown in Figure 2A. The onset of vaginal cornification was delayed in *Med12$^{fl/fl}$ Amhr2-Cre* mice when compared to control mice (35.60 ± 0.87 vs 30.60 ± 1.29, n = 5, $P < 0.05$, Figure 2B). Along with the delayed onset of vaginal cornification, the age of the first estrous cycle was also delayed in *Med12$^{fl/fl}$ Amhr2-Cre* females when compared to controls (71.20 ± 5.25 vs 55.00 ± 1.70, n = 5, $P < 0.05$, Figure 2B). Furthermore, during the 6-week observation period, the number of estrous cycles was reduced in *Med12$^{fl/fl}$ Amhr2-Cre* females in comparison with those in the control group (1.83 ± 0.54 vs 4.17 ± 0.31, n = 6, $P < 0.01$, Figure 2C). *Med12$^{fl/fl}$ Amhr2-Cre* mice spent more time in the metestrus stage than controls (23.20 ± 1.86 vs 13.60 ± 1.63, n = 5, $P < 0.01$) (Figure 2D). Metestrus stage correlates with decline in estradiol and progesterone levels, and both vaginal cornification and estrous cycle are dependent on circulating estradiol levels [26, 27]. The abnormal estrous cycles indicate problems with steroidogenesis and impaired ovarian function in *Med12$^{fl/fl}$ Amhr2-Cre* mice.

Med12 deficiency disrupts granulosa cell function in the ovary

Ovaries play an essential role in reproductive hormonal physiology, whereby androgen precursors are synthesized by the theca cells and transported to granulosa cells for conversion to estradiol [28]. After ovulation, the remaining follicular tissue forms corpus luteum that secretes high levels of progesterone, and moderate levels of estradiol and inhibin A [29, 30]. We carefully examined ovarian histology in *Med12* conditional knockout mice. We observed normal ovarian histology in *Med12$^{fl/+}$ Amhr2-Cre* mice, with normal appearing follicles, oocytes, granulosa cells, and corpora lutea (Supplementary Figure 2B and E). Abundant corpora lutea were present in both control and *Med12$^{fl/+}$ Amhr2-Cre* mice. However, examination of *Med12$^{fl/fl}$ Amhr2-Cre* ovaries revealed significant histologic abnormalities. Granulosa cells in *Med12$^{fl/fl}$ Amhr2-Cre* mice showed distinct hyperchromatic staining not present in controls, consistent with apoptosis features in the dying follicles (Supplementary Figure 2F). Ovarian histomorphometry showed reduced number of antral follicles in *Med12$^{fl/fl}$ Amhr2-Cre* mice (n = 3, $P < 0.05$, Supplementary Figure 2G) as compared to controls. *Amhr2* promoter-driven *Cre* is highly active in secondary and small antral follicles as opposed to smaller primordial and primary follicles [31]. *Med12* deficiency in these larger follicles likely explains the decreased number of antral

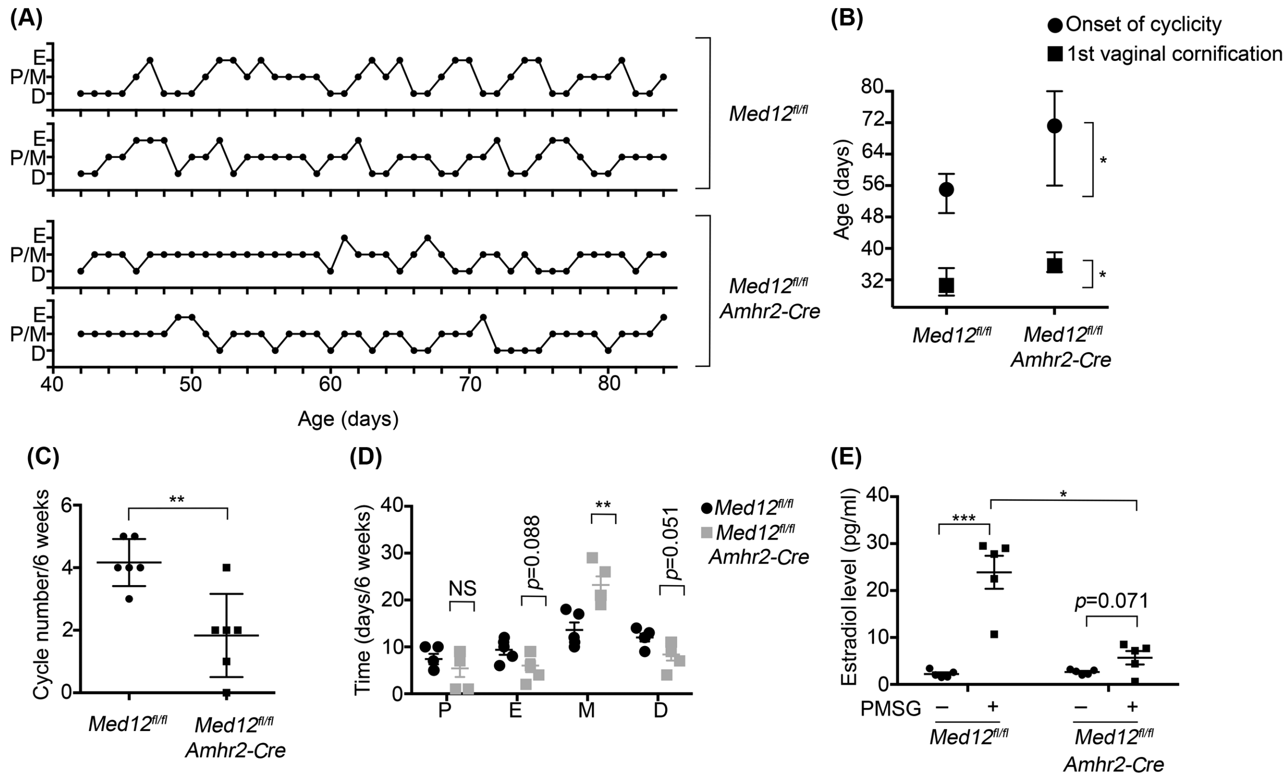

Figure 2. Estrous cycle is disrupted in *Med12^fl/fl^ Amhr2-Cre* mice. (A) Schematic representation of the estrous cycles in *Med12^fl/fl^* and *Med12^fl/fl^ Amhr2-Cre* females. (B) Ages at first vaginal cornification and onset of first cyclicity are plotted against the genotype and shows a delay in *Med12^fl/fl^ Amhr2-Cre* versus *Med12^fl/fl^* (control) mice (n = 5). (C) Number of estrous cycles counted over a 6-week period in *Med12^fl/fl^* and *Med12^fl/fl^ Amhr2-Cre* females (n = 6) shows a significant decrease in *Med12^fl/fl^ Amhr2-Cre* females. (D) Days spent at each stage of the estrous cycle over a 6-week period plotted against each stage (n = 5). Stages are defined as P, proestrus; E, estrus; M, metestrus; D, diestrus. (E) Estradiol concentration was measured in the serum of 3-week-old *Med12^fl/fl^* and *Med12^fl/fl^ Amhr2-Cre* females collected in mice without (–) and with PMSG treatment (+) after 48 h (n = 5). Data are represented as mean ± SEM. $^{*}P < 0.05$ (B, E), $^{**}P < 0.01$ (C, D), $^{***}P < 0.001$ (E).

follicles. Corpora lutea were rarely visualized in *Med12^fl/fl^ Amhr2-Cre* ovaries, arguing that spontaneous ovulation rarely occurred.

We also assessed the response of ovarian follicular development in *Med12^fl/fl^ Amhr2-Cre* and control animals exposed to exogenous pregnant mare serum gonadotropin (PMSG). PMSG stimulated control ovaries, as expected, responded, and developed abundant pre-ovulatory follicles (Figure 3A, C, E, and G, n = 4, $P < 0.001$, Figure 3I). These pre-ovulatory follicles are characterized by the presence of antral fluid and cumulus granulosa cells that surround oocytes [23]. Significantly fewer pre-ovulatory follicles were observed in PMSG-stimulated *Med12^fl/fl^ Amhr2-Cre* ovaries (n = 4, $P < 0.05$, Figure 3I) when compared to controls. These results are consistent with the interpretation that *Med12* deficiency disrupts granulosa cell response to exogenous gonadotropins.

Med12^fl/fl^ Amhr2-Cre mice are infertile and their estrous cycle perturbed, due to disrupted hormonal production from granulosa cells. Since *Med12* is a transcriptional regulator, we assessed expression of granulosa cell transcripts known to be involved in ovarian steroidogenesis. We performed quantitative real-time PCR on genes known to be involved in steroidogenesis. We assayed nuclear receptor subfamily 5, group A, member 2 (*Nr5a2*), follicle stimulating hormone receptor (*Fshr*), luteinizing hormone/choriogonadotropin receptor (*Lhcgr*), cytochrome P450, family 19, subfamily a, polypeptide 1 (*Cyp19a1*), cyclin D2 (*Ccnd2*), estrogen receptor 1 (*Esr1*), and estrogen receptor 2 (*Esr2*). We quantitated downregulation of *Nr5a2*, *Esr1,* and *Esr2* and upregulation of *Lhcgr* (n = 3, $P < 0.5$, Figure 3J). *Nr5a2* and *Lhcgr* are genes that are critical during the development of pre-ovulatory follicles and ovarian luteinization [32–34]. *Esr1* and *Esr2* deficiency is known to disrupt folliculogenesis, corpora lutea formation, and meiotic resumption of pre-ovulatory oocytes [35–37]. It is interesting that transcriptional level of *Ccnd2*, implicated in granulosa cell proliferation [38], was not affected. The disrupted expression of these genes is consistent with reduced ability of *Med12^fl/fl^ Amhr2-Cre* granulosa cells to respond to gonadotropins and synthesize to estradiol [35, 39].

Med12^fl/fl^ Amhr2-Cre mice have abnormal circulating steroid levels

We measured estradiol levels in the serum from 3-week-old mice before and after PMSG stimulation. The basal level of estradiol in control and *Med12^fl/fl^ Amhr2-Cre* mice was not statistically significant prior to PMSG exposure (n = 5, Figure 2E). PMSG induces estradiol synthesis in granulosa cells and promotes maturation of small follicles into larger, pre-ovulatory follicles [40]. Upon the injection of PMSG, there was a sharp increase of estradiol in control mice (n = 5, $P < 0.001$, Figure 2E). However, the estradiol response to PMSG was blunted in *Med12^fl/fl^ Amhr2-Cre* mice and estradiol levels in *Med12^fl/fl^ Amhr2-Cre* mice were significantly lower when compared to control mice (n = 5, $P < 0.05$, Figure 2E). The blunted

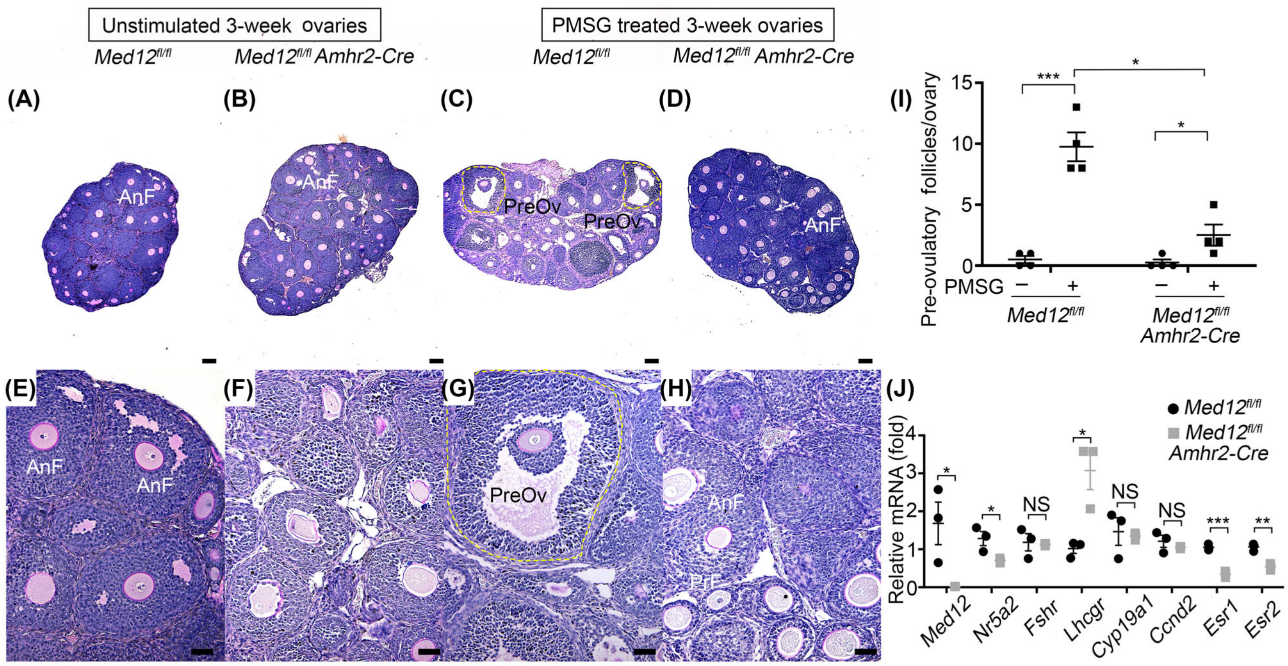

Figure 3. *Med12$^{fl/fl}$ Amhr2-Cre* ovarian response to PMSG stimulation and gene expression. (A–H) *Med12$^{fl/fl}$* and *Med12$^{fl/fl}$ Amhr2-Cre* mice were treated with PMSG for 48 h, and ovaries were sectioned and stained by periodic acid-Schiff. Representative histology is shown in panels (A–H), comparing unstimulated and PMSG stimulated 3-week-old ovaries. Significantly more pre-ovulatory follicles were present in the *Med12$^{fl/fl}$* control group after PMSG treatment as compared to *Med12$^{fl/fl}$ Amhr2-Cre* group. AnF, antral follicles; Gr, granulosa cells; PreOv, pre-ovulatory follicles. Scale bars = 100 μm. (I) Quantification of pre-ovulatory follicles from 3-week-old *Med12$^{fl/fl}$* and *Med12$^{fl/fl}$ Amhr2-Cre* females treated with or without PMSG for 48 h (n = 4). (J) Granulosa cells were isolated from PMSG-treated *Med12$^{fl/fl}$* and *Med12$^{fl/fl}$ Amhr2-cre* ovaries (n = 3), and RNA was extracted for cDNA conversion and real-time quantitative polymerase chain reaction (RT-qPCR). Data were normalized to *Gapdh* expression and were given as the mean relative quantity (compared with control), with error bars representing the standard error of the mean. Student *t*-test was used to calculate *P* values. The only significant difference was noted in the expression of *Med12*, as expected, as well as upregulation of *Lhcgr*, and downregulation of *Nr5a2, Esr1,* and *Esr2*. Pooled data represent mean ± SEM. $^*P < 0.05$, $^{**}P < 0.01$, $^{***}P < 0.001$.

response to PMSG is consistent with observed phenotypes of irregular estrus cycles (Figure 2A), and lack of vaginal plugs (Figure 1D) in *Med12$^{fl/fl}$ Amhr2-cre* mice.

Intrinsic uterine defects cannot be rescued by exogenous steroids in *Med12$^{fl/fl}$ Amhr2-Cre* mice

We further examined the uterine anatomy and histology in *Med12$^{fl/+}$Amhr2-Cre*, *Med12$^{fl/fl}$Amhr2-Cre*, and control animals. The 12-week uterine morphology of *Med12$^{fl/+}$ Amhr2-Cre* mice was similar to the control group, and uterine weights were not reduced (n = 7, Figure 4B). The gross morphology in 12-week-old *Med12$^{fl/fl}$ Amhr2-Cre* female mice revealed atrophic uteri (Figure 4A) that weighed significantly less than controls (n = 7, $P < 0.01$, Figure 4B). The histology of the *Med12$^{fl/+}$ Amhr2-Cre* and control uteri (Figure 4D and G) revealed distinct endometrial and myometrial layers (Figure 4C and F). In contrast, endometrium and myometrium layers were hypoplastic in the *Med12$^{fl/fl}$ Amhr2-Cre* uteri (Figure 4E and H).

The uterus is highly sensitive to estradiol and progesterone levels. The abnormal steroidogenesis in *Med12$^{fl/fl}$ Amhr2-Cre* mice may explain the hypoplastic uterine phenotype in *Med12$^{fl/fl}$ Amhr2-Cre* mice. To determine whether uterine hypoplasia in *Med12$^{fl/fl}$ Amhr2-Cre* mice is solely due to abnormal steroidogenesis or whether *Med12* intrinsically disrupts uterine development, we implanted placebo and steroid pellets in 4-week-old ovariectomized *Med12$^{fl/fl}$* (control) and *Med12$^{fl/fl}$ Amhr2-Cre* mice. After 4 weeks of exogenous steroids, the uteri of control and *Med12$^{fl/fl}$ Amhr2-Cre* mice were collected for histological analysis. The estradiol and progesterone concentrations reached similar levels in both control and *Med12$^{fl/fl}$ Amhr2-Cre* ovariectomized mice (n = 4, Figure 5A and B). Estradiol pellets rescued the weight of both ovariectomized control and *Med12$^{fl/fl}$ Amhr2-Cre* uteri to 50% of the nonovariectomized wild-type uterus (n = 5, Figure 5C). Estradiol and progesterone combined pellet implantation completely rescued the weight of control uteri but only partially rescued weights of the *Med12$^{fl/fl}$ Amhr2-Cre* uteri, reaching 50% of the control group (n = 5, $P < 0.0001$, Figure 5C). The size difference between the control and *Med12$^{fl/fl}$ Amhr2-cre* uteri exposed to combined estradiol and progesterone implants was significant (Figure 5D). These results demonstrate that exogenous steroids did not fully rescue the *Med12$^{fl/fl}$ Amhr2-Cre* uterine size nor weight, and that *Med12$^{fl/fl}$ Amhr2-Cre* uterine response to estradiol combined with progesterone was blunted. Examination of histology revealed that ovariectomized control and *Med12$^{fl/fl}$ Amhr2-Cre* mice treated with placebo implants had atrophic layers of endometrium and myometrium, as expected (Figure 5E). After the implantation of estradiol or combined estradiol/progesterone implants, control uteri recovered well-developed endometrial and myometrial compartments, with an increase in the cytoplasmic portion of the cells in each layer (Figure 5E). Unlike controls, *Med12$^{fl/fl}$ Amhr2-Cre* uteri did not show well-developed endometrial and myometrial layers when exposed to exogenous estradiol or combined estradiol/progesterone implants. Moreover, *Med12$^{fl/fl}$ Amhr2-Cre* uteri exposed to estradiol and progesterone implants displayed abnormal

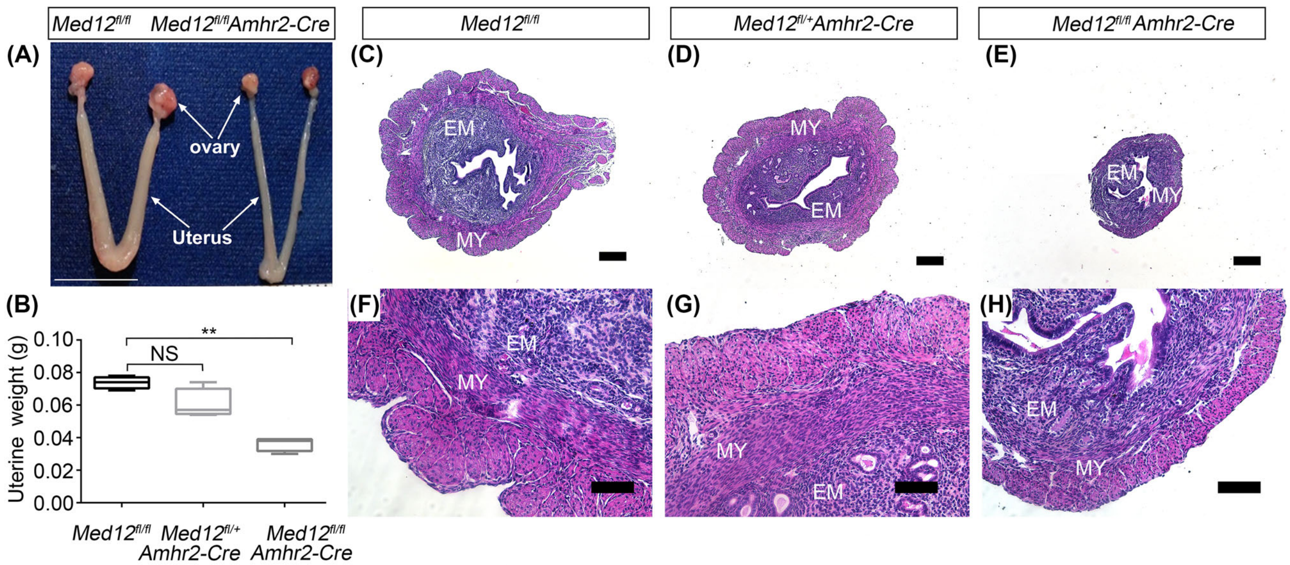

Figure 4. *Med12$^{fl/fl}$ Amhr2-Cre* uterine anatomy and histology. (A) Gross morphology of 12-week-old female mouse reproductive tract. The *Med12$^{fl/fl}$* (control mice) display normal reproductive tract. In comparison to the controls, *Med12$^{fl/fl}$ Amhr2-Cre* reproductive tract is atrophic. Scale bar = 1cm. (B) Twelve-week-old uterine weight is significantly decreased in *Med12$^{fl/fl}$ Amhr2-Cre* as compared to *Med12$^{fl/fl}$* and *Med12$^{fl/+}$ Amhr2-Cre* group (n = 7). Data are presented as mean ± SEM. $^{**}P < 0.01$. (C–H) Hematoxylin and eosin staining of uteri from 12-week-old *Med12$^{fl/fl}$*, *Med12$^{fl/+}$ Amhr2-Cre* and *Med12$^{fl/fl}$ Amhr2-Cre* mice synchronized with PMSG and hCG. Note the atrophic uteri of *Med12$^{fl/fl}$ Amhr2-Cre* female. EM, endometrium; MY, myometrium. Scale bars = 100 μm.

histology consisting of intramyometrium glandular structures (Figure 5E). These results are consistent with the interpretation that *Med12$^{fl/fl}$ Amhr2-Cre* uterine hypoplasia is not solely due to disrupted steroid production in granulosa cells, but also due to intrinsic uterine defects.

We examined expression of genes known to be important in uterine development in control and *Med12$^{fl/fl}$ Amhr2-Cre* uteri. We assayed gene expression in three groups of uteri: (1) uteri from ovariectomized animals implanted with placebo pellets, (2) ovariectomized animals implanted with estradiol pellets, and (3) ovariectomized animals implanted with combined estradiol/progesterone pellets. We specifically examined expression of steroid receptors, *Esr1*, *Esr2,* and progesterone receptor (*Pgr*) (*PR-AB*) and one of the isoforms *PR-B*, as well as genes downstream of steroid receptors such as G protein-coupled estrogen receptor 1 (*Gper1*), notch 1 (*Notch1*), and Smoothened, Frizzled Class Receptor (*Smo*). *Esr1* is the key mediator of estrogen action on uterine growth [41]. There was no significant change of *Esr1* expression between ovariectomized *Med12$^{fl/fl}$ Amhr2-Cre* mice and the control group before steroid supplementation. Estradiol implants, as expected, downregulated *Esr1* in both groups (n = 3, $P < 0.001$, Supplementary Figure 3A). The combined estradiol and progesterone implants further suppressed *Esr1* expression in controls (n = 3, $P < 0.01$), but failed to further reduce *Esr1* expression in *Med12$^{fl/fl}$ Amhr2-Cre* uteri (n = 3, $P < 0.05$, Supplementary Figure 3A). *Esr2* expression was not significantly different between controls and *Med12$^{fl/fl}$ Amhr2-Cre* uteri under different experimental conditions (n = 3, Supplementary Figure 3B). The expression of *Pgr* was lower in ovariectomized *Med12$^{fl/fl}$ Amhr2-Cre* mice when compared to control uteri (n = 3, $P < 0.05$, Supplementary Figure 4A). Estradiol or combined estradiol/progesterone implants rescued *Pgr* expression in both *Med12$^{fl/fl}$ Amhr2-Cre* and control uteri to similar levels (n = 3, Supplementary Figure 4A). The progesterone receptor isoform *PR-B* expression was lower in *Med12$^{fl/fl}$ Amhr2-Cre* ovariectomized uterus compared to control uterus (n = 3, $P < 0.05$) and was rescued by estradiol or estradiol combined progesterone supplementation in both control and *Med12$^{fl/fl}$ Amhr-Cre* uteri (n = 3, Supplementary Figure 4B). These results suggest that expressions of progesterone receptors in *Med12$^{fl/fl}$ Amhr2-Cre* uteri can be rescued by exogenous steroids.

We also examined genes that are downstream of the estradiol and progesterone pathways, and implied in promoting or inhibiting uterine growth. Insulin-like growth factor 1 (*Igf1*), Kruppel-like factor 15 (*Klf15*), zinc finger and BTB domain containing 16 (*Zbtb16*), and Indian Hedgehog (*Ihh*) expression was similar under the three experimental conditions in both *Med12$^{fl/fl}$ Amhr2-Cre* and control uteri. *Igf1* is a mediator of estradiol actions in uterine cells [42]. *Igf1* expression was upregulated in both *Med12$^{fl/fl}$ Amhr2-Cre* and control uteri treated with estradiol (n = 3, $P < 0.0001$) or combined estradiol and progesterone treatment (n = 3, $P < 0.0001$, Supplementary Figure 3C). *Klf15*, *Zbtb16,* and *Ihh* are known to be uterine growth inhibitors [43–45]; the expression of these inhibitory factors was similarly reduced in steroid-exposed *Med12$^{fl/fl}$ Amhr2-Cre* and control mice (*Klf15,* n = 3, $P < 0.001$, Supplementary Figure 3C; *Zbtb16*, n = 3, $P < 0.01$, Supplementary Figure 4C; *Ihh*, n = 3, $P < 0.05$, Supplementary Figure 4D). *Gper1* and nuclear receptor subfamily 2, group F, member 2 (*Nr2f2*), were significantly more downregulated in the ovariectomized *Med12$^{fl/fl}$ Amhr2-Cre* uterus as compared to the control (n = 3, $P < 0.05$), but estradiol (n = 3, $P < 0.0001$) or estradiol combined with progesterone treatment (*Gper1*, n = 3, $P < 0.01$) suppressed the expression to the same level in control and *Med12$^{fl/fl}$ Amhr2-Cre* uteri (*Gper1*, Figure 5F; *Nr2f2*, Supplementary Figure 4E). *Gper1* is a known estrogen receptor mediating *ERK1/2* signaling pathway in uterine tissue [46], and it is known to be downregulated by estradiol in uterine smooth muscle tissues [47]. *Nr2f2* can inhibit the uterine epithelium proliferation [44]. These results indicate that at the baseline, there is abnormal *Nr2f2* and *Gper1* expression in *Med12$^{fl/fl}$ Amhr2-Cre* uteri. The misexpression

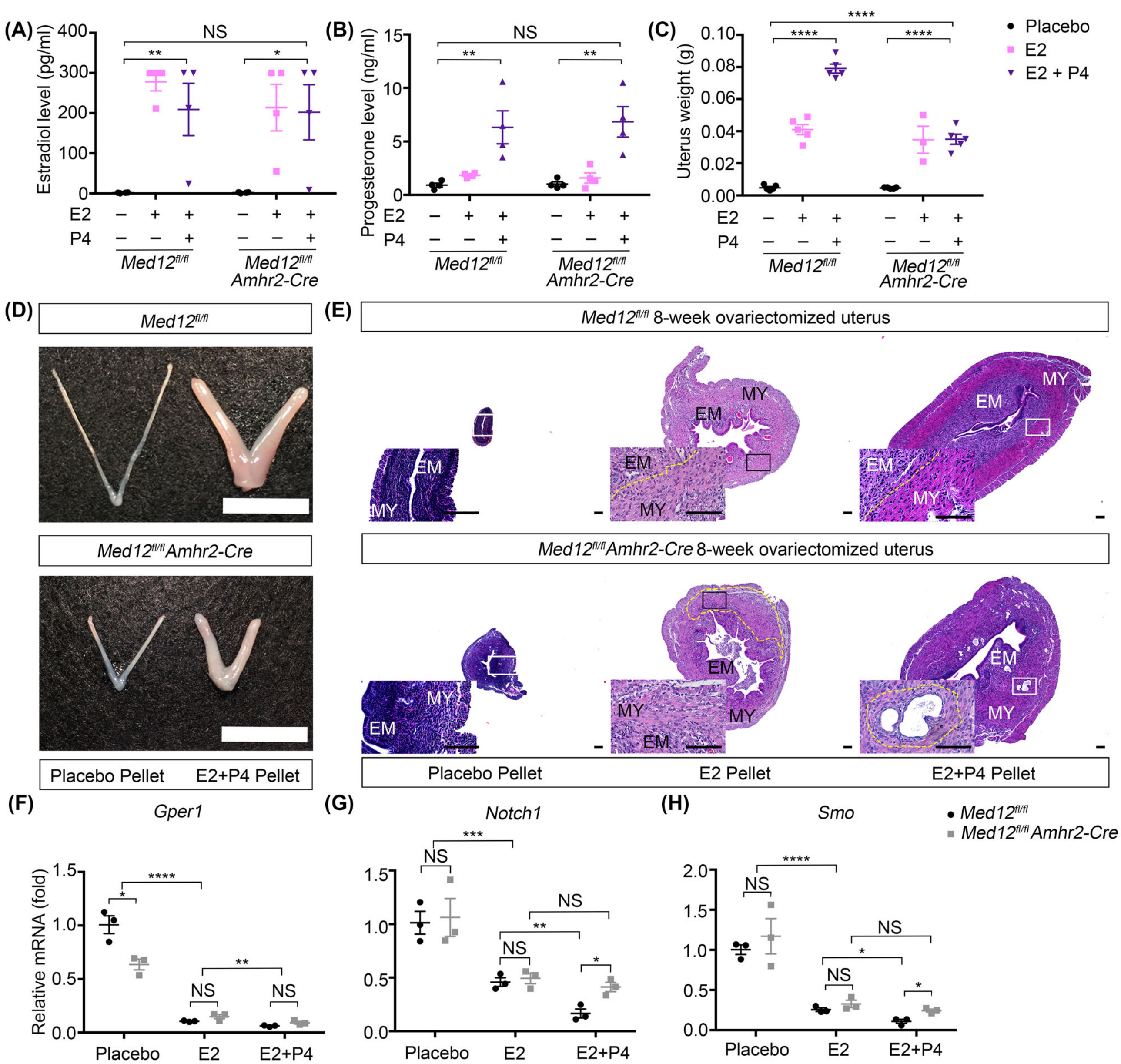

Figure 5. Exogeneous estradiol and progesterone cannot fully rescue the uterine hypoplasia in *Med12fl/fl Amhr2-Cre* mice. (A, B) Serum estradiol (A) and progesterone (B) concentrations were measured in ovariectomized *Med12fl/fl* and *Med12fl/fl Amhr2-Cre* mice after the implantation of placebo, estradiol, or estradiol combined with progesterone pellets for 4 weeks (n = 4). (C) Uterine weights in ovariectomized *Med12fl/fl* and *Med12fl/fl Amhr2-Cre* mice implanted with placebo, estradiol, or estradiol combined with progesterone pellets for 4 weeks (n = 5). (D) Gross morphology of uteri from 8-week-old ovariectomized *Med12fl/fl* and *Med12fl/fl Amhr2-Cre* mice implanted with placebo and estradiol combined with progesterone pellets for 4 weeks. Note significant increase in uterine size after exposure to combined estradiol and progesterone pellets. (E) Hematoxylin & eosin staining of uteri from 8-week-old ovariectomized *Med12fl/fl* (control) and *Med12fl/fl Amhr2-Cre* mice implanted with, placebo, estradiol, or estradiol combined with progesterone pellets for 4 weeks. Zoomed panels are shown below and to the left of the displayed histology section. Placebo treatment had little effect on ovariectomized control and *Med12fl/fl Amhr2-Cre* uteri, with atrophic layers of endometrium and myometrium. After the implantation of estradiol or combined estradiol/progesterone implants, control uteri recovered well-developed endometrial and myometrial compartments (dotted yellow line). Unlike controls, *Med12fl/fl Amhr2-Cre* uteri did not show well-developed endometrial and myometrial layers when exposed to exogenous estradiol or combined estradiol/progesterone implants (dotted yellow line). Moreover, *Med12fl/fl Amhr2-Cre* uteri exposed to estradiol and progesterone implants displayed abnormal histology consisting of intramyometrium glandular structures (dotted yellow line). (F–H) Real-time quantitative polymerase chain reaction (RT-qPCR) on RNA isolated from uteri exposed to placebo, estradiol only, or estradiol and progesterone pellets. Results are shown for *Gper1*, *Notch1,* and *Smo* transcripts (n = 3). Pooled data represent mean ± SEM. $^{*}P < 0.05$ (A, F, G, H); $^{**}P < 0.01$ (A, B, F, G); $^{***}P < 0.001$ (G); $^{****}P < 0.0001$ (C, F, H). MY, myometrium; EM, endometrium. Scale bars = 100 μm.

of *Nr2f2* and *Gper1* was normalized once *Med12*$^{fl/fl}$ *Amhr2-Cre* uteri received exogenous estradiol or estradiol combined with progesterone. *Notch1*, *Smo,* and Patched 1 (*Ptch1*) were genes whose expression differed between controls and *Med12*$^{fl/fl}$ *Amhr2-Cre* mice after exogenous steroid implants. *Notch1* is a known inhibitory factor in uterine development [48]. *Smo* activation impedes uterine differentiation [49]. *Ptch1* is known to inhibit estrogen signaling via paracrine loop [44], halting the growth of uterine epithelium. *Notch1*, *Smo,* and *Ptch1* were downregulated when the uterus was stimulated by exogenous estradiol in both *Med12*$^{fl/fl}$ *Amhr2-Cre* and control groups (*Notch1*, n = 3, $P < 0.001$, Figure 5G; *Smo*, n = 3, $P < 0.0001$, Figure 5H; *Ptch1*, n = 3, $P < 0.0001$, Supplementary Figure 4F). However, in the presence of combined estradiol and progesterone implants, the expression of *Notch1*, *Smo,* and *Ptch1* went lower in the control group (*Notch1*, n = 3, $P < 0.01$, Figure 5G; *Smo*, n = 3, $P < 0.05$, Figure 5H; *Ptch1*, n = 3, $P < 0.001$, Supplementary Figure 4F) but remained unchanged in *Med12*$^{fl/fl}$ *Amhr2-Cre* uteri. These results show that progesterone addition had differing effects on *Notch1*, *Smo,* and *Ptch1* expression in *Med12*$^{fl/fl}$ *Amhr2-Cre* mice when compared to controls. These differences may explain why progesterone had no additional effects on weight rescue of *Med12*$^{fl/fl}$ *Amhr2-Cre* uteri (Figure 5C).

Med12 is a maternal effect gene

The role of *Med12* in oogenesis has not been previously examined. To evaluate its role in oogenesis, we used oocyte-specific *Gdf9-Cre* and *Zp3-Cre* transgenic mice to ablate *Med12* from primordial and primary follicles, respectively. Both primordial and primary follicles form in postnatal ovaries, when majority of oocytes have arrested in diplotene stage of meiosis I. *Gdf9-Cre* and *Zp3-Cre* are highly efficient in recombining loxP sites in oocytes [50–53]. *Gdf9-Cre* males crossed with *Med12*$^{fl/fl}$ females did not produce pups that carried *Gdf9-Cre* (Figure 6A and D). Leaky, paternal *Gdf9-Cre* expression is known to occur, and the sperm carrying *Gdf9-Cre* transgene probably leads to efficient recombination of *Med12* floxed sites in the fertilized egg with subsequent embryo death. This interpretation is consistent with current understanding that paternal and maternal X chromosome are active immediately after fertilization, and biallelic expression of certain genes from both paternal and maternal X chromosomes is required for first few cell divisions to proceed [54]. The lack of *Med12*$^{fl/+}$ *Gdf9-Cre* pups argues for the importance of early embryonic biallelic *Med12* expression for successful embryogenesis to occur. We also utilized *Zp3-Cre*, which is not expressed in the male germline. *Zp3-Cre* males crossed with *Med12*$^{fl/fl}$ females produced *Med12*$^{fl/+}$ *Zp3-Cre* females (Figure 6A and E), again supporting our conclusion that leaky *Gdf9-Cre* from the paternal mating inactivated maternally floxed *Med12* allele. However, when *Med12*$^{fl/+}$ *Zp3-Cre* females were crossed with *Med12*$^{fl/y}$ males, no pups of *Med12*$^{-/fl}$, *Med12*$^{fl/fl}$, *Med12*$^{-/fl}$ *Zp3-Cre*, *Med12*$^{fl/fl}$ *Zp3-Cre*, *Med12*$^{-/y}$, *Med12*$^{fl/y}$, *Med12*$^{-/y}$ *Zp3-Cre*, and *Med12*$^{fl/y}$ *Zp3-Cre* genotypes were born (Figure 6A and F). In these crosses, the *Zp3-Cre* expressed from the female side inactivated floxed *Med12* allele in the oocyte and therefore no *Med12*$^{-/fl}$ pups were born, consistent with requirement for biallelic expression of *Med12* during early development. We successfully generated *Med12*$^{fl/fl}$ *Zp3-Cre* female pups by mating *Med12*$^{fl/y}$ *Zp3-cre* males with *Med12*$^{fl/fl}$ females (Figure 6A and G). *Med12*$^{fl/fl}$ *Zp3-Cre* females were infertile when mated with stud males. The ovarian histology of *Med12*$^{fl/fl}$ *Zp3-Cre* females showed normal folliculogenesis and the presence of normal corpora lutea, indicating successful ovulation (Figure 6B and C). These results indicate that postnatal *Med12* expression in the oocyte is not important for oogenesis, but is essential for early embryo development. *Med12* is therefore a maternal effect gene.

Discussion

MED12 is a critical subunit of the mediator complex, and has an important role in regulating RNA polymerase II transcription. *MED12* global knockout is lethal and shows the importance of *MED12* in early cell growth, differentiation, and development [11, 55]. Human germline mutations in *MED12* associate with several diseases. The germline mutations, predominantly in the carboxyl terminal domain of the MED12 protein, cause X-linked recessive syndromes (Opitz-Kaveggin, Lujan-Fryns, and Ohdo syndrome). Phenotypes include intellectual disability, dysmorphology, and multi-organ structural birth defects [56]. Recently, whole-exome sequencing approaches to various tumors such as fibroadenomas, phyllodes, leiomyomas [12–15], prostate, and adrenocortical carcinomas [16, 17] have associated specific *MED12* variants with these benign and malignant tumors. In the reproductive tract, unique *MED12* variants were identified in exon 2 in approximately 70% of uterine fibroids. Recent studies show that these *MED12* variants in exon 2 are likely to cause uterine leiomyomas via gain-of-function genetic mechanisms [20]. Specific roles of *MED12* in the reproductive tract have not been previously studied in detail. In this manuscript, we utilized well-characterized *Cre* transgenic lines to cause conditional deficiency of *Med12* in a variety of reproductive tissues. We utilized *Amhr2-Cre* to cause *Med12* deficiency in both granulosa cells and uterine mesenchyme. *Med12*$^{fl/+}$ *Amhr2-Cre* females, with one floxed *Med12* locus, are subfertile and *Med12*$^{fl/fl}$ *Amhr2-Cre* mice, with two floxed *Med12* loci, are infertile, consistent with dose-dependent effect of *Med12* deficiency in the female reproductive system. Interestingly, *Amhr2-Cre*-induced deficiency in male mice (*Med12*$^{fl/y}$ *Amhr2-Cre*) did not significantly affect fertility. *Amhr2-Cre* in male reproductive tissues is expressed in Sertoli and Leydig cells [25], and our results suggest that *Med12* has sexual dimorphic effects in both male and female reproductive tracts. *Amhr2-Cre* has been previously shown to efficiently excise loxp sites in both ovaries and testes and has been used in the past to show detrimental effects of another transcriptional regulator, GATA binding protein 4 (*Gata4*), on male infertility [20, 31, 57, 58]. It is possible that *Med12* interactions are tissue and cell type specific. For example, *Med12* in vivo deletion abrogates P300 interaction at enhancers of key hematopoietic genes [59]. The sexually dimorphic effects of *Med12* need further investigation.

The abnormal mating behavior of the *Med12*$^{fl/fl}$ *Amhr2-Cre* females was the primary cause of female infertility and likely due to the abnormal estrous cycle. This conclusion was derived from the lack of vaginal plugs, late onset of vaginal cornification, and delayed onset of estrous cyclicity in *Med12*$^{fl/fl}$ *Amhr2-Cre* females. Although the basal level of estradiol in control and *Med12*$^{fl/fl}$ *Amhr2-Cre* females was similar (Figure 2E), *Med12*$^{fl/fl}$ *Amhr2-Cre* females had inadequate rise in estradiol levels after PMSG stimulation. *Med12*$^{fl/fl}$ *Amhr2-Cre* females have decreased number of antral follicles and after PMSG stimulation, decreased number of pre-ovulatory follicles. Because large antral and pre-ovulatory follicles are the major source of estradiol [28], we cannot exclude a contribution of the decreased number of these follicles toward the impaired PMSG stimulated synthesis of estradiol. These data together indicate that ovarian estradiol production is defective in mice with granulosa cell-specific knockout of *Med12*. Although developing ovarian follicles

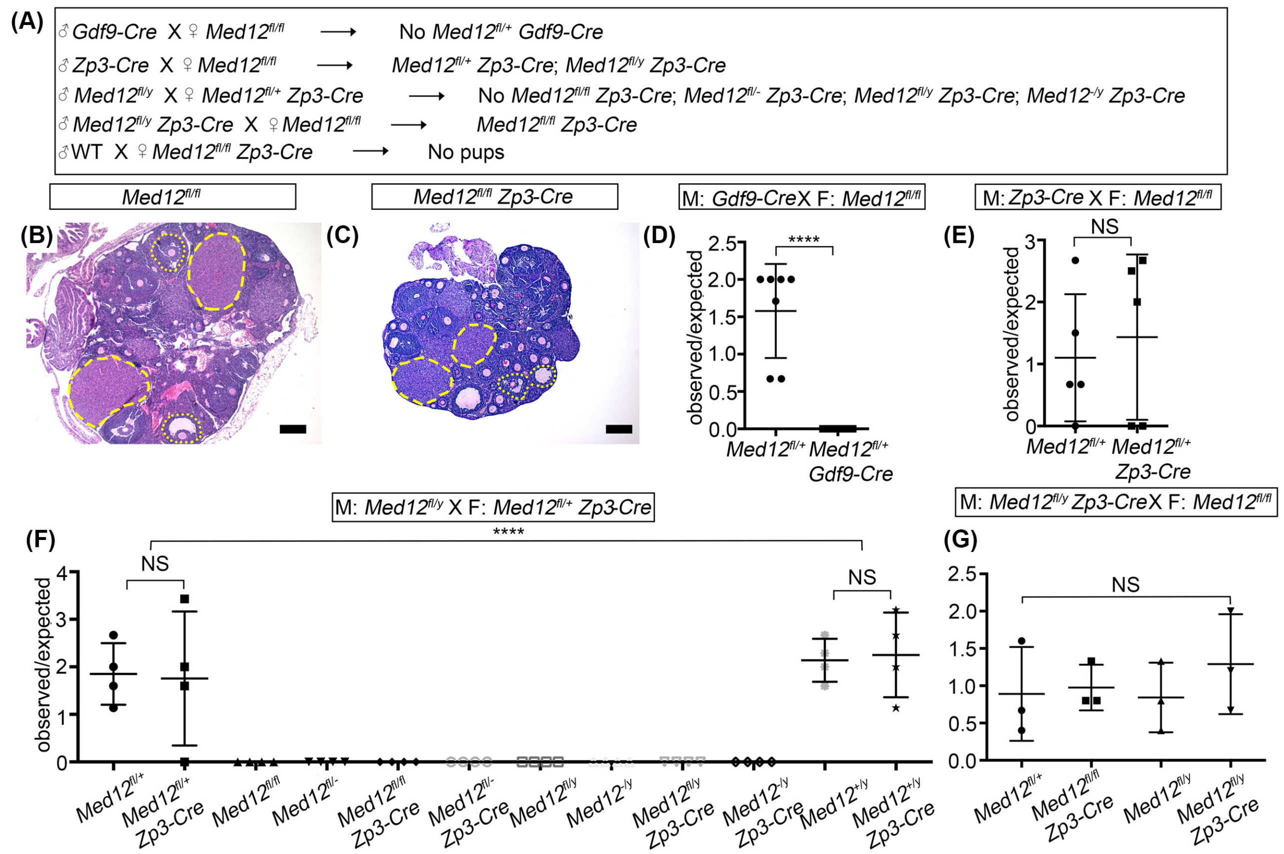

Figure 6. Oocyte-specific deletion of *Med12* causes infertility without affecting folliculogenesis. (A) Breeding strategy used to assess the effects of *Med12* deficiency on folliculogenesis with *Gdf9-Cre* that is active in oocytes of primordial (smallest) ovarian follicles, and *Zp3-Cre* that is active in oocytes of primary follicles. *Gdf9-Cre* introduced from the male side never produced *Gdf9-Cre* positive pups likely due to leaky *Gdf9-Cre* expression from the paternal side that inactivated *Med12* floxed allele from the maternal side and caused embryonic lethality (D). (B, C) Periodic acid-Schiff staining of 12-week-old $Med12^{fl/fl}$ and $Med12^{fl/fl}$ *Zp3-Cre* ovaries generated in crosses described in (A). Note the presence of normal follicles at all stages as well as corpora luteua in both $Med12^{fl/fl}$ and $Med12^{fl/fl}$ *Zp3-Cre* mice. $Med12^{fl/fl}$ *Zp3-Cre* mice are infertile. (D–G) Fertility results from various breeding strategies depicted in (A) are shown. Note lack of mortality when *Zp3-Cre* is transmitted from the male side (G) as opposed to *Gdf9-Cre* (D) (D, n = 7; E, n = 5; F, n = 4; G, n = 3). $^{****}P < 0.0001$. Scale bars = 100 μm.

are the main source of estradiol, other tissues (e.g. adipose tissue) can produce estradiol. The normal basal estradiol level in *Med12* conditional knockout mice may derive from these other sources or maybe due to incomplete *Amhr2-Cre* activity. *Amhr2-Cre* activity depends on the locus in question, and previous work has shown it to be a robust *Cre*, with over 50% recombination [60]. It is therefore likely that the phenotypes we describe here are due to a mosaicism of cells with nonrecombined and recombined genotype. $Med12^{fl/fl}$*Amhr2-Cre* mice mating behavior was disrupted despite PMSG/HCG cycle synchronization, possibly due to dysfunctional granulosa cells and poor rise in estradiol following stimulation as shown in Figure 2E. Alternatively, AMH signaling may have functional significance in the pituitary and hypothalamus, and *Amhr2*-driven deletion of *Med12* in the brain may contribute to anovulation [61, 62].

Within ovarian follicles, theca cells synthesize androgen precursors under stimulation by LH, which the granulosa cells then convert to estradiol [28]. Our conditional knockout via *Amhr2-Cre* will cause *Med12* deficiency in granulosa cells. The histology of $Med12^{fl/fl}$ *Amhr2-Cre* ovaries showed that granulosa cells were abnormal, with many hyperchromatic cells indicative of apoptosis, the number of antral follicles was significantly decreased, and the number of corpora lutea was also significantly lower. *Med12* depletion downregulates the expression of important components of the steroidogenesis pathway, including *Nr5a2*, *Esr1*, and *Esr2*. *Nr5a2* is involved in steroidogenesis, luteinization, and progesterone synthesis [34]. *Esr1* deficiency and *Esr2* deficiency are known to disrupt folliculogenesis [63]. $Med12^{fl/fl}$ *Amhr2-Cre* mice showed less antral follicles and after PMSG stimulation, less pre-ovulatory follicles, which is similar to the ovarian phenotype in *Esr2*-deficient mouse model [36, 64]. *Esr1*-deficient mice have abnormal response to PMSG by upregulating *Lhcgr* and *Cyp19a1*. Granulosa cells of *Esr2*-deficient animals fail to respond to PMSG, in part by upregulating *Fshr* [64]. Interestingly, aromatase (*Cyp19a1*), an essential enzyme in steroidogenesis, and *Fshr*, an important gonadotrophin receptor for follicular growth, were not significantly affected by *Med12* deficiency. Recent studies reveal that *MED12* depletion significantly reduces the estradiol-induced *ESR1* target genes in MCF7 breast cancer cell line [10] and *MED12* mutations, likely gain-of-function mutations, correlate with higher *ESR2* expression in the stromal cytoplasm of fibroadenoma and phyllodes [65]. Collectively, these results suggest that the granulosa cells with specific *Med12* deficiency do not respond properly to PMSG stimulation both in terms of expression of certain critical genes (*Nr5a2*, *Esr1*, and *Esr2*) and in terms of estradiol biosynthesis. This inability presumably reflects a primary ovarian defect that results from the absence of *Med12* expression in the granulosa cells.

Amhr2 promoter-driven *Cre* expression is well known to occur in uterine mesenchymal cells and has been used by multiple investigators to assess the effects of conditional gene deficiency in the uterus [66–68]. In our study, conditional deficiency of *Med12* in the uterus caused uterine atrophy with hypoplasia of the myometrium and endometrium. The hypoplasia was in part due to the abnormal steroidogenesis in *Med12$^{fl/fl}$ Amhr2-Cre* females, and exogenous steroid implants partially rescued *Med12$^{fl/fl}$ Amhr2-Cre* uterine weight.

Both estradiol and progesterone play an important role in uterine morphology during the estrous cycle. Estrogen binds to estrogen receptors, which allows cells to be responsive to progesterone and progesterone receptor. The actions of progesterone and its receptor were shown in multiple studies to be critical for uterine epithelial proliferation and interactions with stromal cells [44]. Our results suggest that progesterone pathways are more disrupted than estrogen pathways in the *Med12*-deficient mouse. We base this conclusion on estradiol only versus combined estradiol and progesterone response in ovariectomized *Med12$^{fl/fl}$ Amhr2-Cre* mice. Estradiol only implants had similar effect on the uterine weights of ovariectomized *Med12$^{fl/fl}$ Amhr2-Cre* and control uteri. Combination of estradiol and progesterone completely rescued uterine weights of control group further. However, no additional benefit of estradiol combined with progesterone was observed in *Med12$^{fl/fl}$ Amhr2-Cre* uterus. *Med12$^{fl/fl}$ Amhr2-Cre* uterus phenotype is similar to the phenotype observed in *Pgr* knockout mouse model [69, 70]. However, *Pgr* and *PR-B* expression was not disrupted in estradiol and estradiol combined with progesterone supplemented *Med12$^{fl/fl}$ Amhr2-Cre* uteri. Therefore, we suspect that *Med12* deficiency could act on genes downstream of *Pgr*. We examined *Pgr* downstream genes including *Zbtb16*, *Ihh*, *Nr2f2*, *Ptch1*, *Notch1,* and *Smo*, along with downstream genes of estrogen receptor, *Klf15*, *Igf1,* and *Gper1*. Progesterone-regulated genes showed abnormal expression in *Med12$^{fl/fl}$ Amhr2-Cre* uteri, either before the exogenous administration of steroids (*Nr2f2*) or after exogenous administration of estradiol combined with progesterone (*Ptch1*, *Notch1*, *Smo*). When activated by *Pgr*, *Ihh* with *Wnt* ligands will induce the expression of *Ptch1* and *Nr2f2*. The subsequent action of *Ptch1* and *Nr2f2* is to antagonize the mitogenic pathways related to growth factors, impeding further uterine epithelial proliferation [44]. It is interesting that *Ptch1* is affected, given that *Amhr2-Cre* is not active in uterine epithelium, which argues that the cross talk between the mesenchyme and epithelium may be disrupted. *Notch1* expression is also dysregulated in *Med12$^{fl/fl}$ Amhr2-Cre* uteri. *Notch1* is known to regulate *Pgr* via epigenetic modifications [48], and *Med12* deficiency could indirectly affect epigenetic modification via disrupting *Notch1* expression. Alternatively, MED12 and PGR proteins physically interact and affect progesterone related pathways, a hypothesis that requires further testing. Our data are also important in the study and treatment of uterine leiomyomas. Traditional treatment, targeting estrogen or progesterone inhibition, needs to be maintained to prevent recurrence [71]. From our studies, progesterone-regulated pathways could be significantly impacted by *Med12* mutation-positive leiomyomas [72]. *Med12*-deficient uterine phenotype observed here is likely milder due to partial *Amhr2* driven *Cre* activity [20]. Our interpretation assumes that *Med12* actions are primarily at the level of transcription, and that transcript levels correlate with protein levels and functions.

Med12 global knockout is embryonic lethal at E10.5 [11]. These results indicate that *Med12* is critical for early embryonic development. However, the role of *Med12* in oocyte differentiation and growth is unknown. Our results from *Gdf9-Cre* and *Zp3-Cre*-mediated *Med12* deficiency are consistent with the conclusion that *Med12* is a maternal effect gene. During early embryogenesis, paternal X chromosomes are active immediately after fertilization, and expression of certain genes is required from both paternal and maternal X chromosomes for development to proceed [54]. *Med12* is expressed from the X chromosome and oocyte-specific *Med12* deficiency from either maternal or paternal germline results in infertility, indicating the necessity of bi-allelic *Med12* expression for early embryogenesis, despite normal ovarian folliculogenesis and oocyte maturation. Few maternal effect genes have been characterized to date, and include genes such as zygote arrest 1 (*Zar1*), DNA methyltransferase (cytosine-5) 1 (*Dnmt1*), developmental pluripotency-associated 3 (*Dppa3*), and NLR family, pyrin domain containing 5 (*Nlrp5*) [73–76]. The characteristic of maternal effect genes to date is that its deficiency has no effect on oogenesis, but is essential for early postfertilization events, and causes one or two-cell embryo arrest. *Med12* behaves as an X chromosome derived maternal effect gene. It is interesting that *Zp3-Cre* driven *Med12* deficiency has no effect on the growing oocytes. Mediator complexes transmit signals from the transcription factors to the polymerase in a variety of tissue [77]. Transcriptional regulation is important for oocyte growth at the primary oocyte stage, as previously shown by disruption of LIM homeobox protein 8 (*Lhx8*) expression [78]. It is therefore interesting that *Med12,* unlike oocyte-specific transcriptional regulators such as *Lhx8*, spermatogenesis and oogenesis specific basic helix-loop-helix 1 (*Sohlh1*), spermatogenesis and oogenesis specific basic helix-loop-helix 2 (*Sohlh2*), and folliculogenesis specific basic helix-loop-helix (*Figla*)*,* is not important during oogenesis and oocyte maturation [78–80]. Whether other members of the mediator complex play a role in oogenesis remains to be determined.

We have demonstrated that the somatic or germline loss of *Med12* causes infertility without evidence for tumorigenesis. *Med12* variants in humans associate with a wide range of tumors and in the reproductive tract, nearly 70% of uterine leiomyomas [81, 82] carry unique *Med12* somatic variants [18, 19]. Our studies further support previous findings [20] that leiomyomas are not caused by the loss of function, but rather by the gain-of-function mutations in the *Med12* gene. The role of *Med12* in the reproductive tract is pleiotropic, disrupting function of various tissues. In the granulosa cells, *Med12* disrupts steroidogenesis; in the uterus, it disrupts uterine development; and in the germline, *Med12* is an X-chromosome gene essential for early embryogenesis. The effects of *Med12* appear to be cell type and tissue specific, and further studies are needed to elucidate *Med12* mechanisms behind reproductive-specific phenotypes caused by *Med12* deficiency.

Supplementary data

Supplementary data are available at *BIOLRE* online.

Supplementary Figure S1. Fertility data of *Med12$^{fl/y}$ Amhr2-Cre* mice. (A) Fertility data of *Med12$^{fl/y}$* (controls, n = 7) and *Med12$^{fl/y}$ Amhr2-Cre* (male conditional knockout, n = 16) males. Males were mated with *Med12$^{fl/fl}$* females for 6 months. (B) Distribution of pups of various genotypes from the mating of *Med12$^{fl/y}$ Amhr2-Cre* males with *Med12$^{fl/fl}$* females. Note that the number of female pups is significantly lower than the number of male pups. Pooled data are represented as mean ± SEM. $^{*}P < 0.05$ (A, B), by Student two-tailed t-test (A, B) and two-way ANOVA (B).

Supplementary Figure S2. ***Med12$^{fl/fl}$ Amhr2-Cre*** **mice have abnormal folliculogenesis.** (A–F) Periodic acid-Schiff staining of 12-week-old female ovaries from *Med12$^{fl/fl}$*, *Med12$^{fl/+}$ Amhr2-Cre*, and *Med12$^{fl/fl}$ Amhr2-Cre* groups. Note the hyperchromatically stained granulosa cells co-occurring with dying follicles, outlined in yellow (F). PrF, primary follicles; SF, secondary follicles; CL, corpus luteum; AnF, antral follicles; Gr, granulosa cells; Oo, oocytes. Scale bars = 100 μm. (G) Quantification of ovarian follicle types in 6-week-old *Med12$^{fl/fl}$* and *Med12$^{fl/fl}$ Amhr2-Cre* mice. Three pairs of ovaries were embedded in paraffin and serially sectioned at 5 μm thickness. The follicles were counted by every fifth section. We scored primary follicles (PrF), secondary follicles (SF), and antral follicles (AnF). Data are represented as mean ± SEM. $^{*}P < 0.05$(G).

Supplementary Figure S3. Expression of estrogen receptors and downstream genes can be partially rescued by exogenous steroids in *Med12$^{fl/fl}$ Amhr2-Cre* uterus. (A–E) Real-time quantitative polymerase chain reaction (RT-qPCR) shows the expression of *Esr1*, *Esr2*, *Igf1,* and *Klf15* mRNAs in uterus isolated from ovariectomized *Med12$^{fl/fl}$* and *Med12$^{fl/fl}$ Amhr2-Cre* mice after the implantation of placebo, estradiol, or estradiol combined with progesterone pellets (n = 3). Pooled data represent mean ± SEM. $^{*}P < 0.05$ (A); $^{**}P < 0.01$ (A, B, C, D); $^{***}P < 0.001$ (A, D); **** $P < 0.0001$ (C) by Student two-tailed *t*-test.

Supplementary Figure S4. Expression of progesterone receptors and downstream genes cannot be fully rescued by exogenous steroids in *Med12$^{fl/fl}$ Amhr2-Cre* uterus. (A–E) Real-time quantitative polymerase chain reaction (RT-qPCR) shows the expression of *Pgr*, *PR-B*, *Zbtb16*, *Ihh*, *Nr2f2,* and *Ptch1* mRNAs in uterus isolated from ovariectomized *Med12$^{fl/fl}$* and *Med12$^{fl/fl}$ Amhr2-Cre* mice after the implantation of placebo, estradiol, or estradiol combined with progesterone pellets (n = 3). Note the expression of *Pgr* and *PR-B* is downregulated by estradiol or estradiol combined with progesterone pellets in both *Med12$^{fl/fl}$* and *Med12$^{fl/fl}$ Amhr2-Cre* group (n = 3, $P < 0.001$). Pooled data represent mean ± SEM. $^{*}P < 0.05$ (A, B, D, E); $^{**}P < 0.01$ (C, F); *** $P < 0.001$ (B, F); $^{****}P < 0.0001$ (C, E, F) by Student two-tailed *t*-test.

Supplementary Table S1. Summary of primers used in Q-PCR analysis of *Med12$^{fl/fl}$ Amhr2-Cre* granulosa cells and ovariectomized uterus.

Acknowledgments

The authors greatly appreciate Dr Heinrich Schrewe and Dr Richard Behringer for donating the mice. The authors thank the Center for Research in Reproduction, University of Virginia School of Medicine, for serum hormone analysis. The authors are grateful to the Magee-Womens Research Institute (MWRI) Animal Core Facility for technical assistance in mouse surgery.

Author contributions

XW contributed to research design, conducting experiments, acquiring and analyzing data, and writing the manuscript. PM contributed to phenotype characterization and data analysis. CC contributed to uterus histology analysis. GR contributed to conducting experiments. AR contributed to design of the research studies, analyzing data, writing and correcting the manuscript, providing the reagents, and handling the revisions.

Conflict of interest: The authors have declared that no conflict of interest exists.

References

1. Conaway RC, Conaway JW. Function and regulation of the Mediator complex. *Curr Opin Genet Dev* 2011;**21**(2):225–230.
2. Borggrefe T, Yue X. Interactions between subunits of the Mediator complex with gene-specific transcription factors. *Semin Cell Dev Biol* 2011;**22**(7):759–768.
3. Bourbon H. Comparative genomics supports a deep evolutionary origin for the large, four-module transcriptional mediator complex. *Nucleic Acids Res* 2008;**36**(12):3993–4008.
4. Philibert RA, Winfield SL, Damschroder-Williams P, Tengstrom C, Martin BM, Ginns EI. The genomic structure and developmental expression patterns of the human OPA-containing gene (HOPA). *Hum Genet* 1999;**105**(1-2):174–178.
5. Samuelsen CO, Baraznenok V, Khorosjutina O, Spahr H, Kieselbach T, Holmberg S, Gustafsson CM. TRAP230/ARC240 and TRAP240/ARC250 Mediator subunits are functionally conserved through evolution. *Proc Natl Acad Sci USA* 2003;**100**(11):6422–6427.
6. Borggrefe T, Davis R, Erdjument-Bromage H, Tempst P, Kornberg RD. A complex of the Srb8, -9, -10, and -11 transcriptional regulatory proteins from yeast. *J Biol Chem* 2002;**277**(46):44202–44207.
7. Knuesel MT, Meyer KD, Donner AJ, Espinosa JM, Taatjes DJ. The human CDK8 subcomplex is a histone kinase that requires Med12 for activity and can function independently of mediator. *Mol Cell Biol* 2009;**29**(3): 650–661.
8. Zhou H, Kim S, Ishii S, Boyer TG. Mediator modulates Gli3-dependent Sonic hedgehog signaling. *Mol Cell Biol* 2006;**26**(23):8667–8682.
9. Zhou H, Spaeth JM, Kim NH, Xu X, Friez MJ, Schwartz CE, Boyer TG. MED12 mutations link intellectual disability syndromes with dysregulated GLI3-dependent Sonic Hedgehog signaling. *Proc Natl Acad Sci USA* 2012;**109**(48):19763–19768.
10. Prenzel T, Kramer F, Bedi U, Nagarajan S, Beissbarth T, Johnsen SA. Cohesin is required for expression of the estrogen receptor-alpha (ESR1) gene. *Epigenetics Chromatin* 2012;**5**(1):13.
11. Rocha PP, Scholze M, Bleiss W, Schrewe H. Med12 is essential for early mouse development and for canonical Wnt and Wnt/PCP signaling. *Development* 2010;**137**(16):2723–2731.
12. Yoshida M, Sekine S, Ogawa R, Yoshida H, Maeshima A, Kanai Y, Kinoshita T, Ochiai A. Frequent MED12 mutations in phyllodes tumours of the breast. *Br J Cancer* 2015;**112**(10):1703–1708.
13. Piscuoglio S, Murray M, Fusco N, Marchiò C, Loo FL, Martelotto LG, Schultheis AM, Akram M, Weigelt B, Brogi E, Reis-Filho JS. MED12 somatic mutations in fibroadenomas and phyllodes tumours of the breast. *Histopathology* 2015;**67**(5):719–729.
14. Pfarr N, Kriegsmann M, Sinn P, Klauschen F, Endris V, Herpel E, Muckenhuber A, Jesinghaus M, Klosterhalfen B, Penzel R, Lennerz JK, Weichert W et al. Distribution of MED12 mutations in fibroadenomas and phyllodes tumors of the breast-implications for tumor biology and pathological diagnosis. *Genes Chromosomes Cancer* 2015;**54**(7):444–452.
15. Mishima C, Kagara N, Tanei T, Naoi Y, Shimoda M, Shimomura A, Shimazu K, Kim SJ, Noguchi S. Mutational analysis of MED12 in fibroadenomas and phyllodes tumors of the breast by means of targeted next-generation sequencing. *Breast Cancer Res Treat* 2015;**152**(2):305–312.
16. Barbieri CE, Baca SC, Lawrence MS, Demichelis F, Blattner M, Theurillat J, White TA, Stojanov P, Van Allen E, Stransky N, Nickerson E, Chae S et al. Exome sequencing identifies recurrent SPOP, FOXA1 and MED12 mutations in prostate cancer. *Nat Genet* 2012;**44**(6):685–689.
17. Assié G, Letouzé E, Fassnacht M, Jouinot A, Luscap W, Barreau O, Omeiri H, Rodriguez S, Perlemoine K, René-Corail F, Elarouci N, Sbiera S et al. Integrated genomic characterization of adrenocortical carcinoma. *Nat Genet* 2014;**46**(6):607–612.
18. Makinen N, Mehine M, Tolvanen J, Kaasinen E, Li Y, Lehtonen HJ, Gentile M, Yan J, Enge M, Taipale M, Aavikko M, Katainen R et al. MED12, the mediator complex subunit 12 gene, is mutated at high frequency in uterine leiomyomas. *Science* 2011;**334**(6053):252–255.

19. Mcguire MM, Yatsenko A, Hoffner L, Jones M, Surti U, Rajkovic A, Shomron N. Whole exome sequencing in a random sample of North American women with leiomyomas identifies MED12 mutations in majority of uterine leiomyomas. *PLoS One* 2012;**7**(3):e33251.
20. Mittal P, Shin Y, Yatsenko SA, Castro CA, Surti U, Rajkovic A. Med12 gain-of-function mutation causes leiomyomas and genomic instability. *J Clin Invest* 2015;**125**(8):3280–3284.
21. Jamin SP, Arango NA, Mishina Y, Hanks MC, Behringer RR. Requirement of Bmpr1a for Müllerian duct regression during male sexual development. *Nat Genet* 2002;**32**(3):408–410.
22. Caligioni CS. Assessing reproductive status/stages in mice. *Curr Protoc Neurosci* 2009; Appendix 4:Appendix 4I.
23. Rajkovic A. NOBOX deficiency disrupts early folliculogenesis and oocyte-specific gene expression. *Science* 2004;**305**(5687):1157–1159.
24. Yuan JS, Reed A, Chen F, Stewart CN. Statistical analysis of real-time PCR data. *BMC Bioinformatics* 2006;**7** (1):85.
25. Tanwar PS, Kaneko-Tarui T, Zhang L, Rani P, Taketo MM, Teixeira J. Constitutive WNT/beta-catenin signaling in murine sertoli cells disrupts their differentiation and ability to support spermatogenesis. *Biol Reprod* 2010;**82**(2):422–432.
26. Nelson JF, Karelus K, Felicio LS, Johnson TE. Genetic influences on the timing of puberty in mice. *Biol Reprod* 1990;**42**(4):649–655.
27. Teixeira RCG, Verna C, Simoes RS, Wolff RB, Baracat EC, Soares-Jr JM. Effects of metoclopramide on the mouse anterior pituitary during the estrous cycle. *Clinics* 2011;**66**(6):1101–1104.
28. Barbieri RL. The endocrinology of the menstrual cycle. *Methods Mol Biol* 2014;**1154**:145–169.
29. Sasano H, Suzuki T. Localization of steroidogenesis and steroid receptors in human corpus luteum. Classification of human corpus luteum (CL) into estrogen-producing degenerating CL, and nonsteroid-producing degenerating CL. *Semin Reprod Med* 1997;**15**(4):345–352.
30. Knight PG, Satchell L, Glister C. Intra-ovarian roles of activins and inhibins. *Mol Cell Endocrinol* 2012;**359**(1-2):53–65.
31. Jorgez CJ, Klysik M, Jamin SP, Behringer RR, Matzuk MM. Granulosa cell-specific inactivation of follistatin causes female fertility defects. *Mol Endocrinol* 2004;**18**(4):953–967.
32. Pelusi C, Ikeda Y, Zubair M, Parker KL. Impaired follicle development and infertility in female mice lacking steroidogenic factor 1 in ovarian granulosa cells. *Biol Reprod* 2008;**79**(6):1074–1083.
33. Fan H-Y, Liu Z, Shimada M, Sterneck E, Johnson PF, Hedrick SM, Richards JS. MAPK3/1 (ERK1/2) in ovarian granulosa cells are essential for female fertility. *Science* 2009;**324**(5929):938–941.
34. Bertolin K, Gossen J, Schoonjans K, Murphy BD. The orphan nuclear receptor Nr5a2 is essential for luteinization in the female mouse ovary. *Endocrinology* 2014;**155**(5):1931–1943.
35. Binder AK, Rodriguez KF, Hamilton KJ, Stockton PS, Reed CE, Korach KS. The absence of ER-beta results in altered gene expression in ovarian granulosa cells isolated from in vivo preovulatory follicles. *Endocrinology* 2013;**154**(6):2174–2187.
36. Emmen JMA, Couse JF, Elmore SA, Yates MM, Kissling GE, Korach KS. In vitro growth and ovulation of follicles from ovaries of estrogen receptor (ER){alpha} and ER{beta} null mice indicate a role for ER{beta} in follicular maturation. *Endocrinology* 2005;**146**(6):2817–2826.
37. Liu W, Xin Q, Wang X, Wang S, Wang H, Zhang W, Yang Y, Zhang Y, Zhang Z, Wang C, Xu Y, Duan E et al. Estrogen receptors in granulosa cells govern meiotic resumption of pre-ovulatory oocytes in mammals. *Cell Death Dis* 2017;**8**(3):e2662.
38. Han Y, Xia G, Tsang BK. Regulation of cyclin D2 expression and degradation by follicle-stimulating hormone during rat granulosa cell proliferation in vitro. *Biol Reprod* 2013;**88**(3):57.
39. Monniaux D. Driving folliculogenesis by the oocyte-somatic cell dialog: lessons from genetic models. *Theriogenology* 2016;**86**(1):41–53.
40. McLean AC, Valenzuela N, Fai S, Bennett SA. Performing vaginal lavage, crystal violet staining, and vaginal cytological evaluation for mouse estrous cycle staging identification. *J Vis Exp* 2012;(67):e4389.
41. Hamilton KJ, Arao Y, Korach KS. Estrogen hormone physiology: reproductive findings from estrogen receptor mutant mice. *Reprod Biol* 2014;**14**(1):3–8.
42. Zhu L, Pollard JW. Estradiol-17beta regulates mouse uterine epithelial cell proliferation through insulin-like growth factor 1 signaling. *Proc Natl Acad Sci USA* 2007;**104**(40):15847–15851.
43. Ray S, Pollard JW. KLF15 negatively regulates estrogen-induced epithelial cell proliferation by inhibition of DNA replication licensing. *Proc Natl Acad Sci USA* 2012;**109**(21):E1334–E1343.
44. Diep CH, Daniel AR, Mauro LJ, Knutson TP, Lange CA. Progesterone action in breast, uterine, and ovarian cancers. *J Mol Endocrinol* 2015;**54**(2):R31–R53.
45. Fahnenstich J. Promyelocytic leukaemia zinc finger protein (PLZF) is a glucocorticoid- and progesterone-induced transcription factor in human endometrial stromal cells and myometrial smooth muscle cells. *Mol Hum Reprod* 2003;**9**(10):611–623.
46. Prossnitz ER, Barton M. The G-protein-coupled estrogen receptor GPER in health and disease. *Nat Rev Endocrinol* 2011;**7**(12):715–726.
47. Tian R, Wang Z, Shi Z, Li D, Wang Y, Zhu Y, Lin W, Gui Y, Zheng X. Differential expression of G-protein-coupled estrogen receptor-30 in human myometrial and uterine leiomyoma smooth muscle. *Fertil Steril* 2013;**99**(1):256–263.e3.
48. Su R, Strug MR, Jeong J, Miele L, Fazleabas AT. Aberrant activation of canonical Notch1 signaling in the mouse uterus decreases progesterone receptor by hypermethylation and leads to infertility. *Proc Natl Acad Sci USA* 2016;**113**(8):2300–2305.
49. Franco HL, Lee KY, Rubel CA, Creighton CJ, White LD, Broaddus RR, Lewis MT, Lydon JP, Jeong J, Demayo FJ. Constitutive activation of smoothened leads to female infertility and altered uterine differentiation in the mouse. *Biol Reprod* 2010;**82**(5):991–999.
50. Smith AL, Kousa YA, Kinoshita A, Fodor K, Yang B, Schutte BC. Generation and characterization of a conditional allele of interferon regulatory factor 6. *Genesis* 2017;**55**.
51. Lan Z, Xu X, Cooney AJ. Differential oocyte-specific expression of Cre recombinase activity in GDF-9-iCre, Zp3cre, and Msx2Cre transgenic mice. *Biol Reprod* 2004;**71**(5):1469–1474.
52. Zhang H, Liu L, Li X, Busayavalasa K, Shen Y, Hovatta O, Gustafsson J, Liu K. Life-long in vivo cell-lineage tracing shows that no oogenesis originates from putative germline stem cells in adult mice. *Proc Natl Acad Sci USA* 2014;**111**(50):17983–17988.
53. Sun Q, Liu K, Kikuchi K. Oocyte-specific knockout: a novel in vivo approach for studying gene functions during folliculogenesis, oocyte maturation, fertilization, and embryogenesis. *Biol Reprod* 2008;**79**(6):1014–1020.
54. Patrat C, Okamoto I, Diabangouaya P, Vialon V, Le Baccon P, Chow J, Heard E. Dynamic changes in paternal X-chromosome activity during imprinted X-chromosome inactivation in mice. *Proc Natl Acad Sci USA* 2009;**106**(13):5198–5203.
55. Graham JM, Schwartz CE. MED 12 related disorders. *Am J Med Genet* 2013;**161A**(11):2734–2740.
56. Online Mendelian Inheritance in Man. Online Mendelian Inheritance in Man. http://omim.org/search/?index=entry&search=Med12&filter=cs_exists%3Atrue&sort=score desc&start=1&limit=10&retrieve=clinicalSynopsis. Accessed May 8, 2017.
57. Jeyasuria P, Ikeda Y, Jamin SP, Zhao L, De Rooij DG, Themmen APN, Behringer RR, Parker KL. Cell-specific knockout of steroidogenic factor 1 reveals its essential roles in gonadal function. *Mol Endocrinol* 2004;**18**(7):1610–1619.
58. Kyronlahti A, Euler R, Bielinska M, Schoeller EL, Moley KH, Toppari J, Heikinheimo M, Wilson DB. GATA4 regulates Sertoli cell function and fertility in adult male mice. *Mol Cell Endocrinol* 2011;**333**(1):85–95.
59. Aranda-Orgilles B, Saldaña-Meyer R, Wang E, Trompouki E, Fassl A, Lau S, Mullenders J, Rocha PP, Raviram R, Guillamot M, Sánchez-Díaz M, Wang K et al. MED12 regulates HSC-specific enhancers independently of mediator kinase activity to control hematopoiesis. *Cell Stem Cell* 2016;**19**(6):784–799.
60. Robker RL, Watson LN, Robertson SA, Dunning KR, Mclaughlin EA, Russell DL, Sun Q. Identification of sites of STAT3 action in the female reproductive tract through conditional gene deletion. *PLoS One* 2014;**9**(7):e101182.

61. Cimino I, Casoni F, Liu X, Messina A, Parkash J, Jamin SP, Catteau-Jonard S, Collier F, Baroncini M, Dewailly D, Pigny P, Prescott M et al. Novel role for anti-Müllerian hormone in the regulation of GnRH neuron excitability and hormone secretion. *Nat Commun* 2016;**7**:10055.
62. Hernandez Gifford JA, Hunzicker-Dunn ME, Nilson JH. Conditional deletion of beta-catenin mediated by Amhr2cre in mice causes female infertility. *Biol Reprod* 2009;**80**(6):1282–1292.
63. Dupont S, Krust A, Gansmuller A, Dierich A, Chambon P, Mark M. Effect of single and compound knockouts of estrogen receptors alpha (ERalpha) and beta (ERbeta) on mouse reproductive phenotypes. *Development* 2000;**127**(19):4277–4291.
64. Couse JF, Yates MM, Deroo BJ, Korach KS. Estrogen receptor-beta is critical to granulosa cell differentiation and the ovulatory response to gonadotropins. *Endocrinology* 2005;**146**(8):3247–3262.
65. Tan WJ, Chan JY, Thike AA, Lim JCT, Md Nasir ND, Tan JSY, Koh VCY, Lim WK, Tan J, Ng CCY, Rajasegaran V, Nagarajan S et al. MED12 protein expression in breast fibroepithelial lesions: correlation with mutation status and oestrogen receptor expression. *J Clin Pathol* 2016;**69**(10):858–865.
66. Daikoku T, Jackson L, Besnard V, Whitsett J, Ellenson LH, Dey SK. Cell-specific conditional deletion of Pten in the uterus results in differential phenotypes. *Gynecol Oncol* 2011;**122**(2):424–429.
67. Ferguson L, Kaftanovskaya EM, Manresa C, Barbara AM, Poppiti RJ, Tan Y, Agoulnik AI. Constitutive Notch signaling causes abnormal development of the oviducts, abnormal angiogenesis, and cyst formation in mouse female reproductive tract. *Biol Reprod* 2016;**94**(3):67.
68. Harman RM, Cowan RG, Ren Y, Quirk SM. Reduced signaling through the hedgehog pathway in the uterine stroma causes deferred implantation and embryonic loss. *Reproduction* 2011;**141**(5):665–674.
69. Goddard LM, Murphy TJ, Org T, Enciso JM, Hashimoto-Partyka MK, Warren CM, Domigan CK, Mcdonald AI, He H, Sanchez LA, Allen NC, Orsenigo F et al. Progesterone receptor in the vascular endothelium triggers physiological uterine permeability preimplantation. *Cell* 2014;**156**(3):549–562.
70. Lydon JP, Demayo FJ, Funk CR, Mani SK, Hughes AR, Montgomery CA, Shyamala G, Conneely OM, O'malley BW. Mice lacking progesterone receptor exhibit pleiotropic reproductive abnormalities. *Genes Dev* 1995;**9**(18):2266–2278.
71. Bulun S, Moravek M, Yin P, Ono M, Coon VJ, Dyson M, Navarro A, Marsh E, Zhao H, Maruyama T, Chakravarti D, Kim J et al. Uterine leiomyoma stem cells: linking progesterone to growth. *Semin Reprod Med* 2015;**33**(5):357–365.
72. Tsigkou A, Reis FM, Lee MH, Jiang B, Tosti C, Centini G, Shen F, Chen Y, Petraglia F. Increased progesterone receptor expression in uterine leiomyoma: correlation with age, number of leiomyomas, and clinical symptoms. *Fertil Steril* 2015;**104**(1):170–175.e1.
73. Dean J, Nelson LM, Tong Z, Gold L, Pfeifer KE, Dorward H, Lee E, Bondy CA. Mater, a maternal effect gene required for early embryonic development in mice. *Nat Genet* 2000;**26**(3):267–268.
74. Wu X, Viveiros MM, Eppig JJ, Bai Y, Fitzpatrick SL, Matzuk MM. Zygote arrest 1 (Zar1) is a novel maternal-effect gene critical for the oocyte-to-embryo transition. *Nat Genet* 2003;**33**(2):187–191.
75. Payer B, Saitou M, Barton SC, Thresher R, Dixon JPC, Zahn D, Colledge WH, Carlton MBL, Nakano T, Surani MA. Stella is a maternal effect gene required for normal early development in mice. *Curr Biol* 2003;**13**(23):2110–2117.
76. Howell CY, Bestor TH, Ding F, Latham KE, Mertineit C, Trasler JM, Chaillet JR. Genomic imprinting disrupted by a maternal effect mutation in the Dnmt1 gene. *Cell* 2001;**104**(6):829–838.
77. Yin J-W, Wang G. The Mediator complex: a master coordinator of transcription and cell lineage development. *Development* 2014;**141**(5):977–987.
78. Pangas SA, Choi Y, Ballow DJ, Zhao Y, Westphal H, Matzuk MM, Rajkovic A. Oogenesis requires germ cell-specific transcriptional regulators Sohlh1 and Lhx8. *Proc Natl Acad Sci USA* 2006;**103**(21):8090–8095.
79. Ren Y, Suzuki H, Jagarlamudi K, Golnoski K, Mcguire M, Lopes R, Pachnis V, Rajkovic A. Lhx8 regulates primordial follicle activation and postnatal folliculogenesis. *BMC Biol* 2015;**13**:39.
80. Shin Y, Ren Y, Suzuki H, Golnoski KJ, Ahn HW, Mico V, Rajkovic A. Transcription factors SOHLH1 and SOHLH2 coordinate oocyte differentiation without affecting meiosis I. *J Clin Invest* 2017;**127**(6):2106–2117.
81. Marshall L, Spiegelman D, Barbieri RL, Goldman MB, Manson JE, Colditz GA, Willett WC, Hunter DJ. Variation in the incidence of uterine leiomyoma among premenopausal women by age and race. *Obstet Gynecol* 1997;**90**(6):967–973.
82. Flake GP, Andersen J, Dixon D. Etiology and pathogenesis of uterine leiomyomas: a review. *Environ Health Perspect* 2003;**111**(8):1037–1054.